Observable consequences of chemical equilibration in energetic heavy ion collisions

Jens Konopka, Harald Graf, Horst Stöcker, and Walter Greiner
Institut für Theoretische Physik, Johann Wolfgang Goethe-Universität, D-60054 Frankfurt am Main, Federal Republic of Germany
(Received 22 February 1994)

The quantum statistical model (QSM) is used to calculate nuclear fragment distributions in chemical equilibrium. Several observable isotopic effects are predicted for intermediate energy heavy ion collisions. It is demonstrated that particle ratios for different systems do not depend on the breakup density—the only free parameter in our model. The importance of entropy measurements is discussed. Specific particle ratios for the system Au+Au are predicted, which can be used to determine the chemical potentials of the hot midrapidity fragment source in nearly central heavy ion collisions.

PACS number(s): 25.70.Pq

I. INTRODUCTION

Heavy ion collisions serve as a powerful tool for investigations concerning the thermal properties of nuclear matter [1–4], because they allow for a systematic variation of parameters, e.g., the system size the projectile and target combination and entropy and temperature by the incident energy.

In the following we consider only symmetric projectile-target combinations. Such a reaction can be viewed as follows: The two heavy nuclei impinging on each other will form a hot and dense region of nuclear matter, which is centered around the center of mass rapidity. Due to the strong compression and the rapid sequence of hard nucleon-nucleon scattering, nucleons will be stopped and then escape from the central reaction zone. During the phase of high pressure projectile and target matter is still streaming in. This hinders the escape of the nucleons from the *participant zone* in the longitudinal direction. Therefore matter is squeezed out of the reaction plane and projectile and target material bounces off in the reaction plane. These collective flow phenomena have been predicted by nuclear hydrodynamics [1,5] and Vlasov-Uehling-Uhlenbeck (VUU) and quantum molecular dynamics (QMD) [6–8] models and have been discovered experimentally [9–13].

As the impact parameter approaches zero, more and more nucleons are part of the central reaction zone. Information about the nuclear equation of state away from the saturation point at $E(\rho = \rho_0 = 0.16\,\mathrm{fm}^{-3}, T = 0) = -16\,\mathrm{MeV/nucleon}$ can be searched for in this zone.

It is one of the crucial questions in heavy ion physics: whether the concept of an equation of state (EOS) is applicable to these conglomerates of nucleons, which evolve from an initially completely nonequilibrated configuration. An equation of state only makes sense in an equilibrium situation. Thermal equilibration especially has been much debated [14,15]. There are two hints that equilibration, at least locally, seems to be a reasonable assumption: Fluid dynamical calculations, which are basically footed on this assumption, are quite successful in explaining various experimental findings. Moreover, temperature fits to energy or momentum spectra of the emitted particles can be utilized to parametrize the measured data [16,17]. Little information is available corresponding to chemical equilibration.

The initially compressed zone will later on expand again, a process which is governed by the freeze-out of clusters. According to hydrodynamics [18] this expansion is almost adiabatic (=isentropic), so that the temperature will drop considerably. This implies that the major fraction of entropy will be created in the early stages of the collision. Although the freeze-out happens in the late stages, these clusters still carry information about the thermodynamical properties of the initially compressed system. The pressure, temperature, entropy, and energy content of the hot and dense medium are the relevant quantities, which have to be deduced in order to learn about the nuclear equation of state. Unfortunately none of them can straightforwardly be measured in an experiment.

However, beside the above mentioned projectile-target combination and the incident energy, there exists a third parameter, to which until now, only minor attention has been paid: The charge to mass or equivalently the N/Z ratio of the system under consideration appears to dominate the nuclear chemistry, in particular at the lower energies. Nevertheless, the N/Z ratio is not expected to play an important role for the gross features of the mass or charge distribution, but it can give a strong impact on the abundances and particle ratios in particular isotopic channels.

Variation of the initial isospin of the combined system should give new insights to the equation of state physics. Numerous infinite matter calculations are done under the stringent condition of symmetric ($N = Z$) nuclear matter. Although the collective effects, i.e., the flow of free neutrons is similar to protons [19], a large neutron excess, which is more likely in heavy nuclei, may have strong impact on the fragmentation of finite nuclear systems.

In principle the fragment distribution could serve as an

indicator for chemical equilibration. However, the information deduced from the cluster yields has to be taken with care, because those fragments which are detected finally will not correspond to a chemical equilibrium configuration. The half-life times of some isotopes of the equilibrated system are short compared to the time scale until the expansion phase has ceased. Therefore, their decay has to be taken into account, which yields final fragment distribution, which does not reveal a chemical equilibrium configuration.

In the following section we will briefly outline the main features of the quantum statistical model (QSM). Then the influence of the isospin of the system on the fragment distributions will be presented. Under the assumption of a large chemically equilibrated source, several predictions on particle yields in symmetric heavy ion collisions are made. Finally a summary of the material is given.

II. THE QUANTUM STATISTICAL MODEL

In the following we briefly describe the quantum statistical model (QSM) [20,21]. It treats the breakup of an excited nuclear system in equilibrium. Such systems may be single excited nuclei as well as some composite bulk of nucleons, which is formed in heavy ion collisions. In principle there are several possibilities for a statistical description of the breakup. All these methods have in common that the filling of the available phase space is calculated, either on average or on the basis of an event by event sampling. It depends on the ensemble used in the particular model. There exists a couple of attempts to probe the microcanonical phase space by means of Metropolis importance sampling method [22–25]. Introducing a temperature rather than a fixed energy of the system, a canonical ensemble has to be simulated [26]. There are various models dealing with the statistical fragmentation of excited nuclei in this manner. However, all these methods need the exact size of the system, which is actually decaying, as an input. Especially in experiments where the high excitation is reached by usage of heavy ions, the initial size is not easily deduced due to preequilibrium effects and the fact that only a part of the nucleons participates in the direct reaction (cf. participant-spectator picture). Competing models [27,28] do not rely on the stringent assumption of an overall equilibrated source, which suddenly breaks into pieces. Here a big, excited nucleus decays by sequential evaporation of light particles and intermediate mass fragments which themselves may further decay, until the excitation energy falls below the threshold for particle emission for each single fragment produced.

QSM operates in the grandcanonical ensemble, i.e., the equilibrium state is characterized by a density and a temperature. Hence, the particle number plays only insofar a role, that the relative abundances may be normalized to a finite size of the total system. Nevertheless, a third variable, namely the N/Z ratio controls the isotopic distribution of the fragments produced.

In fact, QSM calculates the nuclear fragment distribution in complete thermodynamical equilibrium. In its present numerical realization, 961 stable and instable states up to mass 20 are considered. Further stable isotopes up to mass 208 are included in the calculation. The latter are not essential for the outcome of the model as far as the energies are as high as they are in this case. They contribute only little to the equilibrium distribution; more than 99% of the initial mass will be stored in clusters not heavier than $A = 20$.

The calculation consists of finding the protochemical and neutrochemical potentials μ_p and μ_n for a fragment mixture at some density ρ and temperature T. The finite volume of nucleons and fragments is explicitly included in the model. This leads to a effective reduction of the available volume. For each fragment specie the proper statistics (Bose-Einstein or Fermi-Dirac, respectively) is used together with the proper statistical weight. In global chemical equilibrium the chemical potential of fragment specie i is

$$\mu_i = Z_i\mu_p + N_i\mu_n + E_i \ , \tag{1}$$

where Z_i, N_i, and E_i denote the charge, the neutron number, and the total binding energy of this particular state. By integration over the relevant distribution functions one obtains the primordial cluster distribution, which will be distorted due to the decay of the particle instable states among them [29–31]. This decay is carried out by calculating the barrier penetration probability in WKB approximation. The correct phase-space factor is obtained by summation over all possible angular momenta l which can couple with the spin of the ejectile to the total spin j. γ decays are always assumed to end up in the ground state.

III. SYSTEMS IN NUCLEOCHEMICAL EQUILIBRIUM

In the following we consider an idealized scheme: Using the quantum statistical model introduced above, we calculate nuclear fragment distributions emerging from chemically equilibrated sources produced in central reactions of heavy ions at midrapidity or around projectile rapidity in peripheral reactions. Detailed comparisons with measured data can help to determine the extend of equilibration. Furthermore, it will give new information on the nuclear equations of state, namely, on the chemical potentials involved.

A. Entropy deduction from fragmentation data

The possibility of determining the created entropy via measurable observables has been much debated. The QSM has been applied for this purpose: Various observables like the $d_{\rm like}/p_{\rm like}$ ratio [32] or other relative multiplicities of complex fragment up to α's have been related to the baryonic entropy [33–36]. Therefore, the entropy can be deduced indirectly from measurement. However, the final results will depend on the model which actually has been used. Even more so, there are also dependences

on model parameters. In the case of the QSM the most important parameter is the breakup density, i.e., the density at freeze-out. As we will show later on, QSM can make predictions about different particles and systems, predictions that are independent of the freeze-out density used in the calculation.

Recently it has been demonstrated that heavy fragments emerging from the innermost reaction region can be used to "measure" the amount of baryonic entropy [37]. Besides other observables the normalized total multiplicity of charged fragments can be used for an unique S/A determination, nearly independent of the freeze-out density.

The QSM operates in the grandcanonical ensemble. This is well suited for our purposes, since we are interested in comparisons with experimental data, where each detected event is recorded in a limited part of the total phase space. Therefore, even if very restrictive event selection criteria were applied, the number of particles and the total energy detected changes from event to event. To treat this correctly with a microcanonical model [22,23,25] would require one to produce a large number of events and take the average over several microcanonical samples. On the other hand, if equilibration is established, restrictive selection criteria, which select only a few percent of the most violent events with a large number of nucleons involved, will give a sample of events similar to the situation present in a macrocanonical ensemble, provided that the fluctuations are of statistical origin only. The latter is characterized by a volume, a temperature, and the chemical potentials. There are no further assumptions on particle number or energy. The macrocanonical approximation will not provide information about the fluctuations, but predicts *all* ensemble-averaged observables. Even more so, detailed comparisons with a microcanonical code have shown, that finite size effects change the results by a few percent only [38].

B. Nuclear matter at low densities: evidence for a nuclear cluster equation of state

To understand the isospin dependence in detail, we recall that the chemical potential for each individual fragment species i is Eq. (1). The chemical potential can be decomposed into a contribution which is proportional to the mass number of the isotope under consideration and a term which grows linearly with the isospin component

$$T_i^3 = Z_i - \frac{1}{2}A_i = \frac{Z_i - N_i}{2}. \tag{2}$$

If the binding energy is neglected, which is a good approximation especially at higher temperatures and for heavier clusters, such a representation can be established when the chemical potentials μ_p and μ_n are combined into a nucleochemical and isochemical potential:

$$\mu_{\text{nucleo}} = \frac{\mu_p + \mu_n}{2},$$
$$\mu_{\text{iso}} = \mu_p - \mu_n. \tag{3}$$

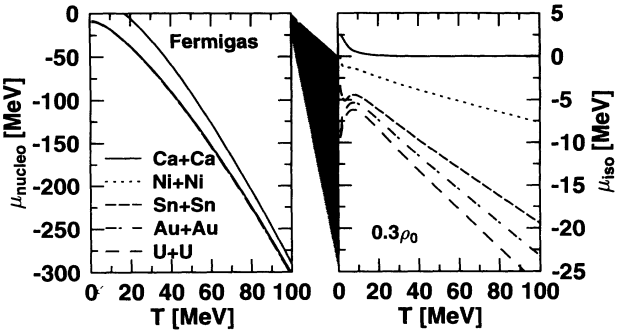

FIG. 1. Nucleochemical and isochemical potential as a function of temperature. Various systems distinguished by their N/Z ratio are displayed. In the $T \to 0$ limit μ_{nucleo} approaches ≈ -8 MeV, the average binding energy of heavy nuclei, rather than +16.5 MeV as for a fourfold degenerated Fermi gas, indicated in the left portion of the figure, at the same density. The breakup density has been kept constant at $0.3\rho_0$. The influence of the isospin becomes less important with increasing temperature—note the different ranges on the μ axes.

Thus the fragment chemical potential reads

$$\mu_i = (Z_i + N_i)\frac{\mu_p + \mu_n}{2} + \frac{Z_i - N_i}{2}(\mu_p - \mu_n) + B_i$$
$$= A_i\mu_{\text{nucleo}} + T_i^3\mu_{\text{iso}} + B_i. \tag{4}$$

The nucleochemical and isochemical potentials can be interpreted as the energy needed to add an additional nucleon to the system and to change the isospin of the system by one unit, respectively. This can be seen in Fig. 1, where μ_{nucleo} and μ_{iso} are shown as a function of the temperature. Different systems differ only as far as the isochemical potential is concerned. The nucleochemical potential is practically equal for all systems regardless of their isospin. As T goes to zero, μ_{nucleo} converges to ≈ -8 MeV. This value is due to the clusterization of complex fragments in low entropy nuclear matter at subsaturation densities as proposed in [39]. In the absence of clusterization, the nucleochemical potential of an equivalent system at the same density (consisting of free protons and neutrons only) is positive, +16.5 MeV.

At the lowest temperatures the binding energy becomes important for the abundance of clusters. Strongly bound clusters will be dominating. The yields will be controlled both by the isospin as well as by the binding energy of the fragments.

Nuclear matter at $T \approx 0$ and at densities below ρ_0 prefers a configuration, where the nucleons are glued together to form heavier clusters [39,40]. Spatial homogenuity is not established on the nucleon level but on a larger scale, where the combined clusters can be regarded as the elementary objects. This interpretation is somewhat density dependent; at the higher densities in particular the lighter clusters immerse in the continuum—the Mott transition in nuclear matter [41,42]. When the temperature is increased, the system behaves more and

more like an ideal Fermi gas of protons and neutrons. The influence of the isochemical potential becomes less important (note the different scales on the axes in Fig. 1).

In addition to the temperature the entropy gained also characterizes the state of the system. Moreover, it nearly stays constant during the expansion phase after a heavy ion collision [18], unlike the temperature, which drops considerably. This is also in accordance with the fact that the temperatures deduced from pion yields or charged particles momentum spectra are too high to be consistent with the large cluster abundances observed. However, an unresolved puzzle remains to be why thermal and chemical equilibrium should be established at different scales.

Although based on observables of the final state of the reaction, the baryonic entropy is connected also to the thermostatic properties of the high density phase. It provides additional information on the overall phase space occupancy in the final stages of heavy ion reactions. This is of special interest, since there is only little information about the mass distribution in configuration space at freeze-out. Therefore, it is important to relate the chemical potentials to the entropy per nucleon in order to show how fragmentation and overall phase space coverage are connected.

As a matter of fact, the primary yield of particle species i is controlled by its fugacity

$$z_i = \exp\left\{\frac{\mu_i}{kT}\right\}, \tag{5}$$

hence the ratio μ/kT is the relevant quantity for the fragmentation. Its entropy dependence is displayed in Fig. 2, where the nucleochemical and the isochemical potential divided by the temperature are shown as a function of the entropy for the systems Ca+Ca, Ni+Ni, Sn+Sn, Au+Au, and U+U. The nucleochemical potential is not influenced by the initial N/Z ratio of the system. This explains the overall similarity in the gross features of the mass distributions regardless of the isospin of the initial system. At rather low temperatures or correspondingly rather low entropies, the isochemical potential and also the related fugacity factor become more important, so that the isospin of the species as well as the mass are of equal relevance for the population.

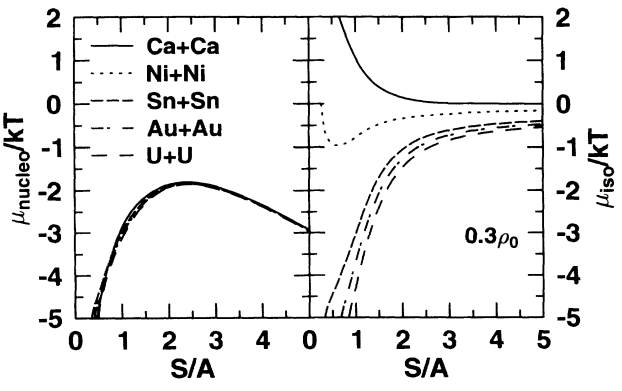

FIG. 2. Nucleochemical and isochemical potential divided by temperature as a function of entropy per nucleon for Ca+Ca, Ni+Ni, Sn+Sn, Au+Au, and U+U systems. The nucleochemical potential does not depend on the initial N/Z ratio of the system.

C. The reduced total fragment multiplicity; link between theory and experimental observations

In order to compare our predictions with experimental data independent of the size of the decaying system, we introduce the reduced total fragment multiplicity $M_{\rm red}$ as the number of the emitted charged products N_c divided by the total charge $Z_{\rm tot}$ of the system. Due to the high complexity of the event shapes and the variety of possible reaction mechanisms, which are partially purely dynamical effects, experimentally the only fragments that have to be considered are those that really stem from regions in phase-space, where the participating nucleons have undergone a sequence of hard collisions and equilibrium may have been established. Unlike previous works, this excludes, e.g., the bounced projectile and target spectators. Therefore the corresponding experimental reduced total fragment multiplicity is defined as

$$M_{\rm red}^{\rm expt} = \left.\frac{\sum_Z n(Z)}{\sum_Z Zn(Z)}\right|_{\rm c.r.r.}, \tag{6}$$

where c.r.r. (= central reaction region) indicates that in some way only particles from the central region are taken into account. This is mandatory since one aims only at those particles which have the highest probability of being chemically equilibrated. Unfortunately, there exists up to now no recipe which provides a proper selection of the participant zone. From the experimental point of view, only angular cuts or cuts in momentum space are applicable. However, these will depend on the specific setup.

Indeed, the quantity $M_{\rm red}$ does not characterize the centrality of the reaction, unlike the absolute multiplicity used in previous experimental analyses. For recent 4π experiments it can be demonstrated that $M_{\rm red}$ does only depend on the incident energy but not on the centrality of the reaction. Our finding suggests that the intensive thermostatic properties of the hot and dense region around midrapidity are essentially controlled by the energy transfer per particle to it—only its total size is determined by the impact parameter. Nevertheless, it is highly appropriate to select only such events with a large participant volume. More peripheral collisions will predominantly feed the bounced spectator, which has been shown to be usable as a barometer of the reaction [43].

In this paper in particular heavy ion collisions in the incident energy range up to 1 GeV/nucleon are considered. The effect of a dynamical change of the N/Z ratio due to pion emission can be neglected below 1 GeV/nucleon. Generally, it is assumed that in the innermost reaction region the N/Z ratio is the same as in the combined projectile-target system.

Different systems are normalized with respect to their total charge rather than to any other possible number like the total mass or neutron number of the system because of several reasons: From the experimental point of view, it is much easier to detect the charge rather than the mass of the emitted fragments. Second, frequently used heavy ion systems have a neutron excess, while almost all produced clusters have masses below 20, where the most stable isotopes have more or less equal proton and neutron numbers. Hence the primary fragment distribution is basically controlled by charge conservation, whereas the conservation of the neutron number is responsible for the abundances in specific isotopic channels. However, the situation is not as clear as that, because many of the primarily produced fragments are particle instable and do undergo decay, which may feed the yields of a particular species to a large extent, which is not in accord with a chemical equilibration of the final fragment distribution.

Figure 3 shows the reduced total fragment multiplicity $M_{\rm red}$ versus the baryonic entropy per nucleon S/A for various systems at a breakup density of $0.3\rho_0$. It is remarkable that the entropy dependence of $M_{\rm red}$ does itself not depend on the N/Z ratio of the initial system. Nevertheless, the relation between incident energy and $M_{\rm red}$, or equivalently the relation between S/A and $E_{\rm lab}$, may be isospin dependent. The former relation $M_{\rm red}(E_{\rm lab})$ can easily be obtained from systematic experimental studies. In particular, for the system Au+Au this excitation function is known; see Table I in [37]. These findings can be used to predict the excitation function of various particle ratios for this system on the basis of the QSM. The range of $M_{\rm red}$ =0.57–0.83 corresponds to laboratory energies from 150 to 800 MeV/nucleon for Au+Au. The values stated depend somewhat on the experimental definition of the central reaction region. Note that even at the higher energies, the amount of fragments is substantial.

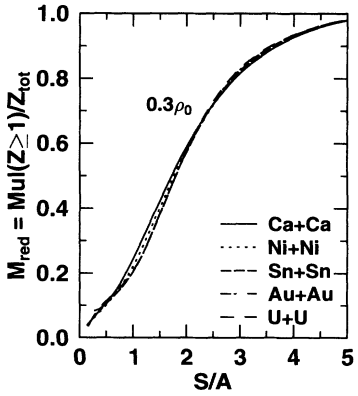

FIG. 3. Reduced total fragment multiplicity as defined in the text as a function of the baryonic entropy for the systems ^{40}Ca+^{40}Ca, ^{56}Ni+^{56}Ni, ^{120}Sn+^{120}Sn, ^{197}Au+^{197}Au, and ^{238}U+^{238}U. A value of $0.3\rho_0$ has been chosen for the freeze-out density. The final fragment distribution is uniquely related to the baryonic entropy of the system, regardless of its N/Z ratio. This behavior is present for all densities.

D. Relative yields of light particles and their ratios—messengers of the nuclear chemistry

This universality with the initial isospin or N/Z ratio encouraged us to use the reduced total fragment multiplicity rather than the entropy as the independent, experimental accessible variable, versus which all other quantities can be plotted. This procedure has the basic advantage that measurable quantities only are used in the corresponding representations, so that the QSM predictions can easily be tested in experiments.

Comparing Fig. 4 left- and right-hand sides, it is apparent that deuterons and α's are of different origin: The former correspond to light particle emission, which is a relevant channel even at the higher energies, e.g., at the AGS [4,44]. On the contrary, the α yield diminishes progressively with increasing $M_{\rm red}$ or incident energy. Obviously the nucleochemical potential is dominating the situation.

As can be seen from Fig. 4, the relative contribution of light particles with equal proton and neutron numbers, where the influence of the isochemical potential is absent, to the total charged particle multiplicity is nearly equal for all systems, independent of the N/Z ratio. This should be different for neutron rich or neutron poor isotopes. For example, provided that chemical equilibrium is achieved to some extent, neutron rich isotopes should be more likely emitted from systems with a high N/Z ratio than from isosymmetric systems. The opposite should be true for neutron poor isotopes. This is illustrated in Fig. 5, where the relative abundances of a neutron rich and a neutron poor isotope, t and ^{3}He, respectively, are plotted versus $M_{\rm red}$. Here it is quantitatively proven that even after the secondary decay of the excited primordial fragments the neutron rich t is more likely produced with systems having a high neutron excess. t is a factor of 2 times more abundant in U+U rather than in Ca+Ca system, whereas in the $N = Z$ case of Ca+Ca ^{3}He is more frequently produced than in the $N > Z$ case of U+U.

Protons are bound in clusters, which do not have the ability to keep the high N/Z ratio of the initial system. This leads to an enhanced production of free neutrons in

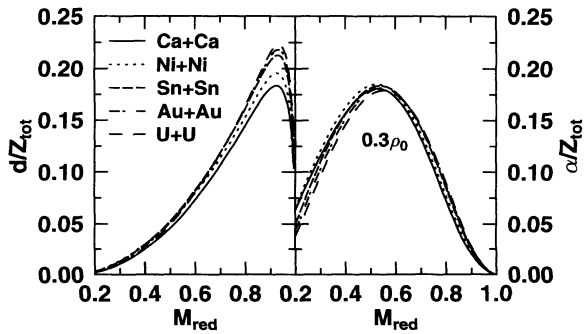

FIG. 4. Relative amount of deuterons (left-hand side) and α particles as a function of the reduced total fragment multiplicity for different systems with varying N/Z ratio.

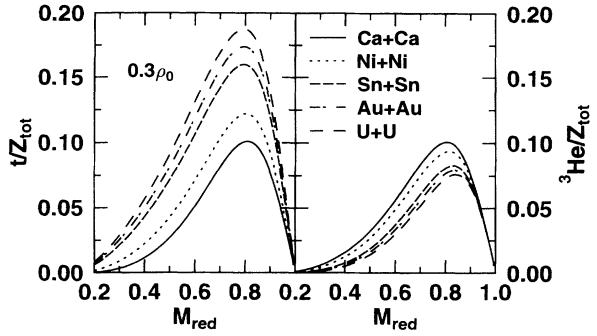

FIG. 5. Relative yields of t and ^{3}He for different systems between Ca+Ca and U+U. A breakup density of $0.3\rho_0$ has been used.

the intermediate energy domain. This behavior will be less pronounced when the N/Z ratio of the initial system is lowered. Moreover, as it can be seen from Fig. 6, right-hand side, for systems which have equal participating proton and neutron numbers, the opposite is true. Here the neutrons are needed in order to glue together the intermediate mass fragments produced. Hence, free protons are emitted more frequently than free neutrons.

The isospin dependence can even more be amplified when considering ratios of yields of neutron rich and neutron poor isotopes. These ratios depend strongly on the chemical composition of the initial system. Moreover, they reveal strong entropy dependence and may therefore serve as a tool for entropy measurements. Additionally, they have the advantage that the volume dependence partially divides out, since the yields are proportional to the available volume. In Fig. 6, right-hand side, this behavior is expressed by the neutron-to-proton ratio which approaches only asymptotically the value expressing the N/Z ratio of the entire system. For the most asymmetric systems, we observe a tremendous neutron enhancement compared to free protons. Taking the measured Au+Au data and assuming a breakup density of $0.3\rho_0$ we predict that 4.3 times more free neutrons than free protons will be emitted from the central reaction zone at 150 MeV/nucleon incident energy. A remarkable result is that this ratio is calculated parameter-free; in particular it is not correlated with the break-up density—the only free parameter in our model. This is expressed in Fig. 6, left-hand side, where n/p is plotted for the system Au+Au using breakup densities between $0.1\rho_0$ and $0.5\rho_0$.

As a matter of fact, from an experimental point of view it is rather difficult to detect neutrons and free protons simultaneously. Nevertheless there exist first experimental observations, which support the prediction of a strong rise of the n/p ratio for systems with a large N/Z ratio as the bombarding energy is lowered [45,46]. Regarding the ratio of the number of neutrons over the number of hydrogen, the strong $M_{\rm red}$ or energy dependence vanishes. As displayed in Fig. 7 for values of $M_{\rm red} > 0.5$ the curves are almost flat for the Ni+Ni as well as the Au+Au case. Nevertheless, this QSM prediction can easily be confronted with the data taken with the LAND device [19] at GSI.

However, the strong isospin dependence is preserved when considering the t over ^{3}He ratio. Similar to the n/p case, here the nucleochemical potentials of both species are equal, but their isospin differs by one unit. A small disturbance enters through the different binding energies of t and ^{3}He, which will become relevant at the lowest temperatures only. The $t/^3$He ratio shows a behavior similar to n/p; see Fig. 8. Large deviations are observed around $M_{\rm red} < 0.7$ from the expectation when the proton-neutron composition of the the initial system is assumed. For systems with a high neutron excess, $t/^3$He exceeds the N/Z ratio of the heavy ions by a factor of 3 and more at the lower energies. This large number demonstrates that the formation of light particles and fragments at these energies cannot be understood in terms of a coalescence picture. This is in agreement with the findings in α-induced reactions at 43 MeV/nucleon [47]. This effect becomes even more drastic when low-

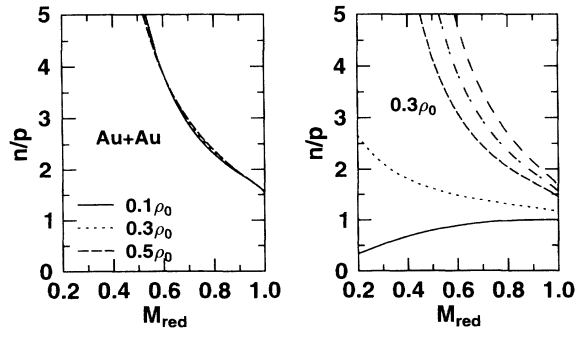

FIG. 6. Free neutron to free proton multiplicity as a function of $M_{\rm red}$. Left-hand side: Dependence of n/p for the Au+Au system on the chosen break-up density. Right-hand side: The corresponding curves are shown for the Ca+Ca, Ni+Ni, Sn+Sn, Au+Au, and U+U systems.

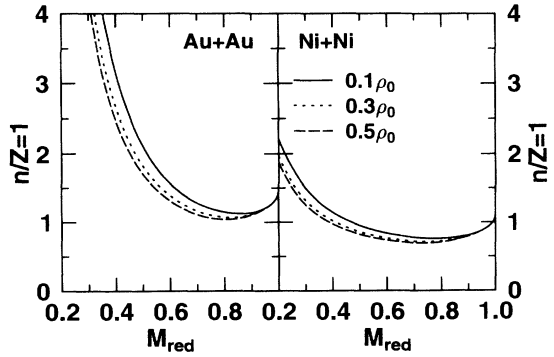

FIG. 7. Neutron-to-hydrogen ratio as a function of $M_{\rm red}$ for reactions of Ni+Ni and Au+Au for breakup densities varying from $0.1\rho_0$ to $0.5\rho_0$.

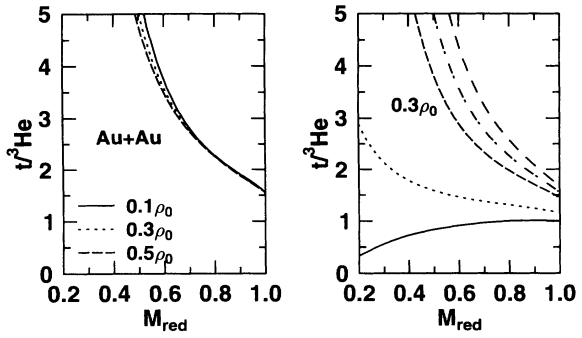

FIG. 8. Same as Fig. 6 for the $t/^3$He ratio.

ering the energy further: Neutrons may be emitted 10 times more frequently than protons.

As the system's isospin goes towards zero (Ni+Ni and Ca+Ca), the incident energy (cf. $M_{\rm red}$ dependence) becomes much weaker, and the n/p and the $t/^3$He ratio reveal the N/Z ratio of the entire system over a wider range of multiplicities. The predicted large differences emerging when considering, e.g., Ca+Ca and U+U could easily be tested in experiments. In addition, our predictions do only weakly depend on the breakup density used in the calculation.

There is another qualitative difference between Ca+Ca and systems with a neutron excess. n/p and $t/^3$He first increase with bombarding energy for Ca+Ca, whereas the ratios decrease for the other system. If the mass of the clusters under consideration increases further, e.g., the ^{6}He-to-^{6}Li ratio, also the Ni+Ni system changes the slope of the energy dependence. This ratio increases for Ni+Ni with $M_{\rm red}$ like in Ca+Ca, but unlike the other ratios (n/p and t^3He) (Fig. 9).

One should be cautious, though, about interpreting measured particle yields directly in terms of a possible chemical equilibration. In the equilibrium calculation a large number of particle instable states have to be taken into account, because their lifetimes are longer than the time scales involved for the equilibration processes. The lifetimes of these isotopes are far too short in order to be detected directly. However, they can be measured by two particle correlations. A wide variety of particle instable states (and γ instable states) has been observed and their abundances are in accordance with the QSM predictions for final temperatures about $T \approx 5$ MeV [48–50]. The final fragment distribution including feeding from instable states does not exhibit the shape of an equilibrium distribution: several components, which participated in the equilibrium configuration have vanished completely. This is a large effect as shown in Fig. 10 and Fig. 11. Here the relative yields of d, α, t, and ^{3}He are plotted in the equilibrium (labeled primordial) and in the final stage. Secondary decays, as mentioned, feed particular channels with multiples of the original yields of this isotope. Thus, it cannot be expected that the initial isospin trivially will have an impact on the final fragment distribution. Such a dependence, although present in the primordial (i.e., equilibrium) stage, does not necessarily need to survive the distortions due to the strong secondary decay effects.

From Fig. 12 it is obvious that this effect is present for nucleons too. In the interesting range $M_{\rm red} = 0.6 - 0.8$ only one-third of the free nucleons in the final stage directly originate from the initial hot and dense region. Therefore the measurement of free nucleons, in particular of free neutrons, gives only partially a direct view into the interesting zone. A large portion of the free nucleon yields is affected by the motion of (excited) fragments plus their nuclear spectroscopy.

Since we know the relation between incident energy and the quantity $M_{\rm red}$ from recent measurements [37], and we have seen that some particle ratios do not depend on the breakup density chosen in our calculations, we can make distinct predictions about the excitation function of these ratios for the Au+Au system. Our predictions concerning the ratios for n/p, $t/^3$He, ^{6}He/^{6}Li are summarized in Table I.

There are several heavy ion experiments in the energy range of interest. Devices which cover almost completely a 4π geometry could address the question to which degree

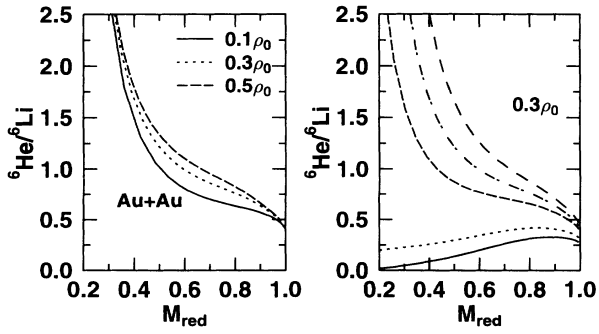

FIG. 9. Same as Fig. 6 for the ^{6}He/^{6}Li ratio.

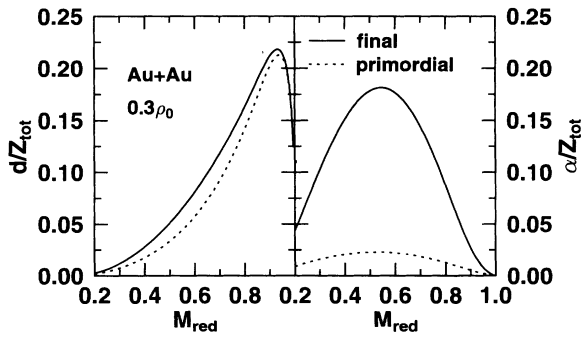

FIG. 10. Relative yields of deuterons and α's as a function of $M_{\rm red}$ for Au+Au at $0.3\rho_0$. Solid lines represent the final distribution, whereas the dotted line shows the primordial distribution before the deexcitation of the particle instable states. The latter corresponds to the chemically equilibrated system.

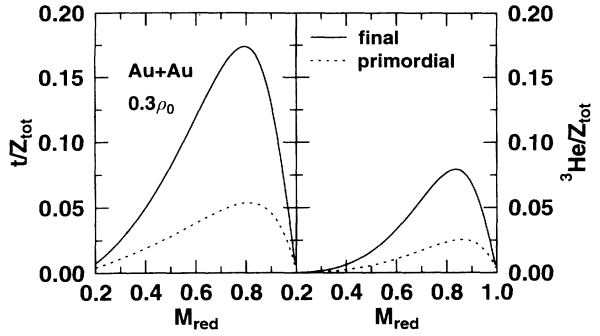

FIG. 11. Same as Fig. 10 but for t and ^{3}He.

TABLE I. Summarized predictions of the quantum statistical model for a selection of particle ratios for Au+Au in the incident energy range from 150 to 800 MeV/nucleon. The excitation function of the reduced total fragment multiplicity is taken from [37]. The extracted numbers only weakly depend on the freeze-out density. The indicated errors correspond to the uncertainty of this parameter. E is in units of MeV/nucleon.

E	$M_{\rm red}$	n/p	$t/^3$He	^{6}He/^{6}Li
150	0.57	4.29 ± 0.04	3.94 ± 0.23	1.05 ± 0.19
250	0.67	3.14 ± 0.05	2.94 ± 0.07	0.89 ± 0.17
400	0.74	2.69 ± 0.06	2.56 ± 0.03	0.82 ± 0.15
600	0.79	2.42 ± 0.05	2.32 ± 0.02	0.77 ± 0.13
800	0.83	2.23 ± 0.04	2.16 ± 0.01	0.73 ± 0.11

chemical equilibrium is established in central reactions of really heavy ions. The physics of thermal and chemical equilibration, the search for a liquid-vapor phase transition [51–53], and the multifragment breakup [54–56] is tightly related to the research program at the Plastic Ball spectrometer [13,34,35], the EOS time projection chamber [57], the FOPI detector at GSI [58], the ALADIN (GSI) + MSU Miniball setup [59], and the forthcoming INDRA detector at GANIL [60]. Unfortunately, data on, e.g., the $t/^3$He ratios at 150 MeV/nucleon Au+Au [13,61] differ by factors of 2–3. However, these data have been obtained in different rapidity bins and *not* over all 4π. The detectors should in the future provide data on the matter for a wider range of phase space.

Equilibrium is indeed a crucial aspect as far as the phenomenon of multifragmentation [54–56] is concerned. Models on multifragmentation often rely on the assumption that the emitting system is equilibrated and the processes can be treated with statistical methods [24,62]. In the past, reasonable agreement between calculations and data has been achieved. It should be mentioned that these models often do not give the event-by-event phase space distribution, even do not analyze data with respect to single source emission. Mass and charge yields can be fairly well reproduced by these type of models. However, as we have demonstrated, a possible chemical equilibration has severe consequences on the isotopic distributions, whereas the mass or charge yields may be less informative. The latter may be explainable in terms of dynamical models like VUU and QMD. On the other hand, in these models fragments are formed via a coalescence mechanism, hence isotope ratios correspond to the combinatorics of the number of protons and neutrons involved. A future experimental confirmation of the details of the predicted enhancement of the various particle ratios with increasing neutron excess in the system would therefore serve as a strong indication for chemical equilibrium. On the contrary, an overall disagreement would point to nonequilibrium processes even in the most violent reactions and would indicate a quest on the applicability of all kinds of equilibrium scenarios as a description of heavy ion reactions.

The most drastic trends are expected at incident energies below 200 MeV/nucleon; see Fig. 13. Using the entropy values obtained with a shock calculation for a

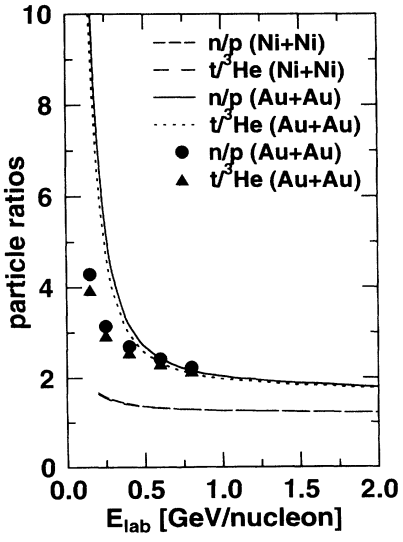

FIG. 12. Excitation function of n/p and $t/^3$He for the Ni+Ni and Au+Au system. Shock calculation of Ref. [63] has been used to extract the entropy as a function of the bombarding energy. These results are shown as lines, whereas the symbols correspond to the predicted ratios using the measured reduced total fragment multiplicities for the system Au+Au.

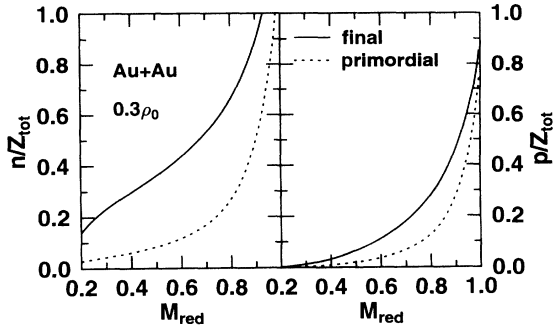

FIG. 13. Primordial and final yields of free nucleons.

equation of state with a compressibility of 270 MeV [63] QSM can also predict the evolution of ensemble averaged observables with bombarding energy. n/p and $t/^3$He particle ratios for the systems Ni+Ni and Au+Au are represented by lines. The symbols correspond to the values summarized in Table I. For the heaviest possible systems with their large neutron excess, the production of free neutrons and neutron rich isotopes, especially the triton, is strongly enhanced. Unfortunately this energy domain is not well covered experimentally up to now. The maximum intermediate mass fragment (IMF) multiplicity is expected between 50 and 150 MeV/nucleon [8]. According to the quantum statistical model, at these rather low incident energies α's should be emitted with a high probability. Depending on the breakup density, at the maximum on the average between 30% and 40% of the total charge will be stored in the α channel (see Fig. 4). Along with the QSM expectations, this should happen even above the energy needed for the maximum IMF production. Thus, heavy ion collisions below $\approx$ 200 MeV/nucleon can shed light on new properties and the decay of excited nuclear matter.

IV. SUMMARY

The quantum statistical model has been applied to study the isospin dependence of fragment production in heavy ion collisions in the few hundred MeV/nucleon incident energy regime. The fragment mass distribution is controlled by the nucleochemical potential and is independent of the initial neutron to proton ratio. On the other hand, in chemical equilibrium the abundances of specific isotopic channels is strongly influenced by this ratio. We have shown that the reduced total fragment multiplicity is correlated to the baryonic entropy in a unique way. The use of $M_{\rm red}$ rather than S/A as the independent variable provides predictions which can be tested experimentally quite easily. In particular, relative particle and light cluster abundances have been calculated for various systems between Ca+Ca and U+U.

The isochemical potential plays a dominant role for particle ratios as n/p, $t/^3$He, and ^{6}He/^{6}Li. It forces systems with a large isospin to a preferential emission of neutron rich isotopes. These ratios do not reveal the original N/Z ratio of the entire system but exceed it by a factor of 2–3 and more at moderate incident energies. It is concluded from this observation that the composite fragment formation cannot be interpreted as a coalescence process.

Several particle ratios are predicted as a function of energy for the system Au+Au. The complete total reduced multiplicity dependence of these ratios for the systems Ca+Ca, Ni+Ni, Sn+Sn, Au+Au, and U+U is provided. Some observables among these, in particular the particle ratios, appear to be independent of the freeze-out density—the only adjustable parameter in the QSM. These observables may therefore serve as an excellent measure of the entropy created in most central heavy ion reactions, if the model predictions are valid.

The forthcoming generation of 4π detectors with the ability for an accurate, simultaneous charge and mass determination will be able to test these predictions experimentally. Detailed comparisons will supply new insights into the (chemical) equilibration process, the chemical potentials, and the absolute amount of entropy produced in heavy ion collisions.

ACKNOWLEDGMENTS

This work was supported by BMFT, DFG, and GSI.

[1] H. Stöcker and W. Greiner, Phys. Rep. **137**, 277 (1986).
[2] R. B. Clare and D. Strottmann, Phys. Rep. **141**, 177 (1986).
[3] *Proceedings on the NATO Advanced Study Institute Programme on The Nuclear Equation of State*, NATO ASI Series B, edited by W. Greiner and H. Stöcker (Plenum, New York, 1990).
[4] *Proceedings on the NATO Advanced Study Institute Programme on Hot and Dense Nuclear Matter*, NATO ASI Series B, edited by W. Greiner and H. Stöcker (Plenum, New York, in press).
[5] W. Scheid, H. Müller, and W. Greiner, Phys. Rev. Lett. **32**, 741 (1974).
[6] J. J. Molitoris and H. Stöcker, Phys. Rev. C **32**, 346 (1985).
[7] J. Aichelin, G. Peilert, A. Bohnet, A. Rosenhauer, H. Stöcker, and W. Greiner, Phys. Rev. C **37**, 2451 (1988).
[8] G. Peilert, H. Stöcker, W. Greiner, A. Rosenhauer, A. Bohnet, and J. Aichelin, Phys. Rev. C **39**, 1402 (1989).
[9] D. Beavis, S. Y. Chu, S. Y. Fun, W. Gorn, A. Huie, D. Keane, J. J. Liu, R. T. Poe, B.C. Shen, and G. vanDalen, Phys. Rev. C. **27**, 2443 (1983).
[10] H. A. Gustafsson, H. H. Gutbrod, B. Kolb, H. Löhner, B. Ludewigt, A. M. Poskanzer, T. Renner, H. Riedesel, H. G. Ritter, A. Warwick, F. Weick, and H. Weimann, Phys. Rev. Lett. **52**, 1590 (1984).
[11] R. E. Renfordt, D. Schall, R. Bock, R. Brockmann, J. W. Harris, A. Sandoval, R. Stock, H. Ströbele, D. Bangert, W. Rauch, G. Odyniec, H. G. Pugh, and L. S. Schröder, Phys. Rev. Lett. **53**, 763 (1984).
[12] K. H. Kampert, J. Phys. G **15**, 691 (1989).
[13] H. H. Gutbrod, A. M. Poskanzer, and H. G. Ritter, Rep. Prog. Phys. **52**, 1267 (1989).
[14] M. Berenguer, C. Hartnack, G. Peilert, H. Stöcker, W. Greiner, J. Aichelin, and A. Rosenhauer, J. Phys. G **18**, 655 (1992).
[15] Dao T. Khoa, N. Ohtsuka, Amand Faessler, M. A. Matin, S. W. Huang, E. Lehmann, and Y. Lotfy, Nucl. Phys. **A542**, 671 (1992).
[16] A. Sandoval, R. Stock, H. E. Stelzer, R. E. Renfordt, J. W. Harris, J. P. Brannigian, J. V. Geaga, L. J. Rosenberg, L. S. Schroeder, and K. L. Wolf, Phys. Rev. Lett. **45**, 874 (1980).
[17] S. Nagamiya, M. C. Lemaire, E. Moeller, S. Schnetzer, G. Shapiro, H. Steiner, and I. Tanihata, Phys. Rev. C **24**, 971 (1981).

[18] W. Schmidt, U. Katscher, B. Waldhauser, J. A. Maruhn, H. Stöcker, and W. Greiner, Phys. Rev. C **47**, 2782 (1993).
[19] Y. Leifels, Th. Blaich, Th. W. Elze, H. Emling, H. Freiesleben, K. Grimm, W. Henning, R. Holzmann, J. G. Keller, H. Klingler, J. V. Kratz, R. Kulessa, D. Lambrecht, S. Lange, E. Lubkiewicz, E. F. Moore, W. Prokopowicz, R. Schmidt, C. Schütter, H. Spies, K. Stelzer, J. Stroth, E. Wajda, W. Waluś, M. Zinser, E. Zude, and the FOPI Collaboration, Phys. Rev. Lett. **71**, 963 (1993).
[20] D. Hahn and H. Stöcker, Phys. Rev. C **37**, 1048 (1988).
[21] D. Hahn and H. Stöcker, Nucl. Phys. **A476**, 718 (1988).
[22] G. Fai and J. Randrup, Nucl. Phys. **A404**, 551 (1983).
[23] G. Fai and J. Randrup, Comput. Phys. Commun. **42**, 385 (1986).
[24] A. S. Botvina and I. N. Mishustin, Phys. Lett. B **294**, 23 (1992).
[25] D. H. E. Gross, Rep. Prog. Phys. **53**, 605 (1990).
[26] D. H. E. Gross and Xiao-ze Zhang, Phys. Lett. **161B**, 47 (1985).
[27] R. J. Charity, M. A. McMahan, G. J. Wozniak, R. J. McDonald, L. G. Moretto, D. G. Sarantites, L. G. Sobotka, G. Guarino, A. Pantaleo, L. Fiore, A. Gobbi, and K. D. Hildenbrand, Nucl. Phys. **A438**, 371 (1988).
[28] M. Blann, T. T. Komoto, and I. Tserruya, Phys. Rev. C **40**, 2498 (1989).
[29] A. Z. Mekijan, Phys. Rev. C **17**, 1051 (1978).
[30] J. Gosset, J. I. Kapusta, and G. D. Westfall, Phys. Rev. C **18**, 844 (1978).
[31] D. Hahn and H. Stöcker, Phys. Rev. C **35**, 1311 (1987).
[32] L. P. Csernai and J. I. Kapusta, Phys. Rep. **131**, 223 (1986).
[33] B. V. Jacak, G. D. Westfall, C. K. Gelbke, L. H. Harwood, W. G. Lynch, D. K. Scott, H. Stöcker, M. B. Tsang, and T. J. M. Symons, Phys. Rev. Lett. **51**, 1846 (1983).
[34] K. G. R. Doss, H. Å. Gustafsson, H. H. Gutbrod, B. Kolb, H. Löhner, B. Ludewigt, A. M. Poskanzer, T. Renner, H. Riedesel, H. G. Ritter, A. Warwick, and H. Wiemann, Phys. Rev. C **32**, 116 (1985).
[35] K. G. R. Doss, H. Å. Gustafsson, H. H. Gutbrod, D. Hahn, K. H. Kampert, B. Kolb, H. Löhner, A. M. Poskanzer, H. G. Ritter, H. R. Schmidt, and H. Stöcker, Phys. Rev. C **37**, 163 (1988).
[36] R. Trockel, K. D. Hildenbrand, U. Lynen, W. F. J. Müller, H. J. Rabe, H. Sann, H. Stelzer, W. Trautmann, R. Wada, E. Eckert, J. Pochodzalla, and N. Brummund, Phys. Rev. C **38**, 576 (1988).
[37] C. Kuhn, J. Konopka, J. P. Coffin, C. Cerruti, P. Fintz, G. Guillaume, A. Houari, F. Jundt, C. F. Maguire, F. Rami, R. Tezkratt, P. Wagner, Z. Basrak, R. Čaplar, N. Cindro, S. Hölbling, J. P. Alard, N. Bastid, L. Berger, S. Boussange, I. M. Belayev, T. Blaich, A. Buta, R. Donà, P. Dupieux, J. Erö, Z. G. Fan, Z. Fodor, R. Freifelder, L. Fraysse, S. Frolov, A. Gobbi, Y. Grigorian, N. Herrmann, K. D. Hildenbrand, S. C. Jeong, M. Jorio, J. Kecskemeti, P. Koncz, Y. Korchagin, R. Kotte, M. Krämer, I. Legrand, A. Lebedev, V. Manko, T. Matulewicz, G. Mgebrishvili, J. Mösner, D. Moisa, G. Montarou, I. Montbel, W. Neubert, D. Pelte, M. Petrovici, S. Ramillien, W. Reisdorf, A. Sadchikov, D. Schüll, Z. Seres, B. Sikora, V. Simion, S. Smolyankin, U. Sodan, K. M. Teh, M. Trzaska, M.A. Vasiliev, P. Wessels, T. Wienold, Z. Wilhelmi, D. Wolfarth, and A. V. Zhilin, Phys. Rev. C **48**, 1232 (1993).
[38] L. P. Csernai, J. I. Kapusta, G. Fai, D. Hahn, J. Randrup, and H. Stöcker, Phys. Rev. C **35**, 1297 (1987).
[39] G. Peilert, J. Randrup, H. Stöcker, and W. Greiner, Phys. Lett. B **260**, 271 (1991).
[40] O. Civitarese, A. Plastino, and A. Faessler, Z. Phys. A **291**, 239 (1979).
[41] G. Röpke, L. Münchow, and H. Schulz, Nucl. Phys. **A379**, 536 (1982); **A399**, 587 (1983).
[42] L. Münchow, H. Schulz, G. Röpke, M. Schlanges, and M. Schmidt, J. Phys. G **8**, L135 (1982).
[43] H. Kruse, B. V. Jacak, and H. Stöcker, Phys. Rev. C **31**, 1770 (1985).
[44] S. Nagamiya and P. Braun-Munzinger (private communication).
[45] W. Schimmeling, J. W. Kast, D. Ortendahl, R. Madey, R. A. Cecil, B. D. Anderson, and A. R. Baldwin, Phys. Rev. Lett. **43**, 1985 (1979).
[46] N. Cindro (private communication).
[47] B. Ludewigt, G. Gaul, R. Glasow, H. Löhner, and R. Santo, Phys. Lett. **108B**, 15 (1982).
[48] J. Pochodzalla, W. A. Friedman, C. K. Gelbke, W. G. Lynch, M. Maier, D. Ardouin, H. Delagrange, H. Doubre, C. Grégoire, A. Kyanowski, W. Mittig, A. Péghaire, J. Péter, F. Saint-Laurent, Y. P. Viyogi, B. Zwieglinski, G. Bizard, F. Lefèbvres, F. Tamain, and J. Québert, Phys. Lett. **161B**, 275 (1985).
[49] M. A. Bernstein, W. A. Friedman, W. G. Lynch, C. B. Chitwood, D. J. Fields, C. K. Gelbke, M. B. Tsang, T. C. Awes, R. L. Ferguson, F. E. Obenshain, F. Plasil, R. L. Robinson, and G. R. Young, Phys. Rev. Lett. **54**, 402 (1985).
[50] C. Schwarz, W. G. Gong, N. Carlin, C. K. Gelbke, Y. D. Kim, W. G. Lynch, T. Murakami, G. Poggi, R. T. de Souza, M. B. Tsang, H. M. Xu, D. E. Fields, K. Kwiatkowski, V. E. Viola, Jr., and S. E. Yennello, Phys. Rev. C **48**, 676 (1993).
[51] J. E. Finn, S. Agarwal, A. Bujak, J. Chuang, J. Gutay, A. S. Hirsch, R. W. Minich, N. T. Porile, R. P. Scharenberg, B. C. Stringfellow, and F. Turkot, Phys. Rev. Lett. **49**, 1321 (1982).
[52] J. Kapusta, Phys. Rev. C **29**, 1735 (1984).
[53] X. Campi, Phys. Lett. B **208**, 351 (1988).
[54] D. R. Bowman, G. F. Peaslee, R. T. de Souza, N. Carlin, C. K. Gelbke, W. G. Gong, Y. D. Kim, M. A. Lisa, W. G. Lynch, L. Phair, M. B. Tsang, C. Williams, N. Colonna, K. Hanold, M. A. McMahan, G. J. Wozniak, L. G. Moretto, and W. A. Friedman, Phys. Rev. Lett. **67**, 1527 (1991).
[55] C. A. Ogilvie, J. C. Adloff, M. Begemann-Blaich, P. Bouissou, J. Hubele, G. Imme, I. Iori, P. Kreutz, G. J. Kunde, S. Leray, V. Lindenstruth, Z. Liu, U. Lynen, R. J. Meijer, U. Milkau, W. F. J. Müller, C. Ngô, J. Pochodzalla, G. Raciti, G. Rudolf, H. Sann, A. Schüttauf, W. Seidel, L. Stuttge, W. Trautmann, and A. Tucholski, Phys. Rev. Lett. **67**, 1214 (1991).
[56] T. C. Sangster, H. C. Britt, D. J. Fields, L. F. Hansen, R. G. Lanier, M. N. Namboodiri, B. A. Remington, M. L. Webb, M. Begemann-Blaich, T. Blaich, M. M. Fowler, J. B. Wilhelmy, Y.D. Chan, A. Dacal, A. Harmon, J. Pouliot, R. G. Stokstad, S. Kaufman, F. Videbaek, Z. Fraenkel, G. Peilert, H. Stöcker, W. Greiner, A. Botvina, and I. Mishustin, Phys. Rev. C **46**, 1404 (1992).

[57] H. G. Ritter, Proccedings of the International School on Nuclear Physics on Heavy Ion Collisions at Intermediate and Relativistic Energies, Erice/Sicily, edited by A. Faessler [Prog. Part. Nucl. Phys. **30**, 1 (1993)].
[58] J. P. Coffin, J. Mod. Phys. E **1**, 739 (1992).
[59] M. B. Tsang, W. C. Hsi, W. G. Lynch, D. R. Bowman, C. K. Gelbke, M. A. Lisa, G. F. Peaslee, G. J. Kunde, M. L. Begemann-Blaich, T. Hofmann, J. Hubele, J. Kempter, P. Kreutz, W. D. Kunze, V. Lindenstruth, U. Lynen, M. Mang, W. F. J. Müller, M. Neumann, B. Ocker, C. A. Ogilvie, J. Pochodzalla, F. Rosenberger, H. Sann, A. Schüttauf, V. Serfling, J. Stroth, W. Trautmann, A. Tucholski, A. Wörner, E. Zude, B. Zwieglinski, S. Aiello, G. Immé, V. Pappalardo, G. Raciti, R. J. Charity, L. G. Sobotka, I. Iori, A. Moroni, R. Scardoni, A. Ferrero, W. Seidel, Th. Blaich, L. Stuttge, A. Cosmo, W. A. Friedman, and G. Peilert, Phys. Rev. Lett. **71**, 1502 (1993).
[60] F. Saint-Laurent and the INDRA Collaboration, *Proceedings of the XXII Workshop on Gross Properties of Nuclei and Nuclear Excitations, Hirschegg, Austria*, edited by H. Feldmeier and W. Nörenberg (GSI, Darmstadt, 1994), p. 162.
[61] G. Poggi, M. Bini, A. Olmi, P. Maurenzig, G. Pasquali, N. Taccetti, P. Danielewicz, and FOPI Collaboration, contribution to [4].
[62] Bao-An Li, A. R. DeAngelis, and D. H. E. Gross, Phys. Lett. B **303**, 225 (1993).
[63] H. Stöcker, M. Gyulassy, and J. Boguta, Phys. Lett. **103B**, 269 (1981).

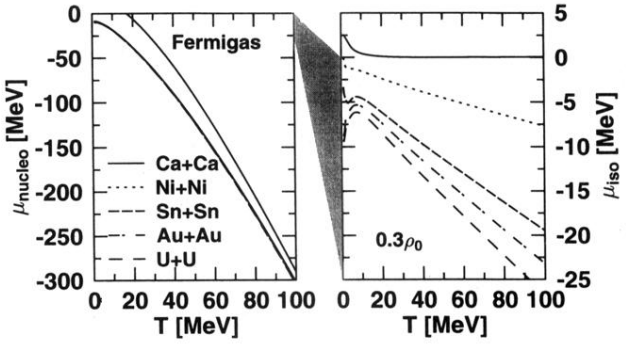

FIG. 1. Nucleochemical and isochemical potential as a function of temperature. Various systems distinguished by their N/Z ratio are displayed. In the $T \rightarrow 0$ limit μ_{nucleo} approaches ≈ -8 MeV, the average binding energy of heavy nuclei, rather than $+16.5$ MeV as for a fourfold degenerated Fermi gas, indicated in the left portion of the figure, at the same density. The breakup density has been kept constant at $0.3\rho_0$. The influence of the isospin becomes less important with increasing temperature—note the different ranges on the μ axes.